Electronic Supplementary Material (ESI) for Dalton Transactions.

Supporting information

Enhancement of Peroxidase-like Activity for Hollow Spherical $Fe_xNi_{1-x}S_2$/SC Nanozyme

Hao Tan, Chen Li, and Zhaodong Nan

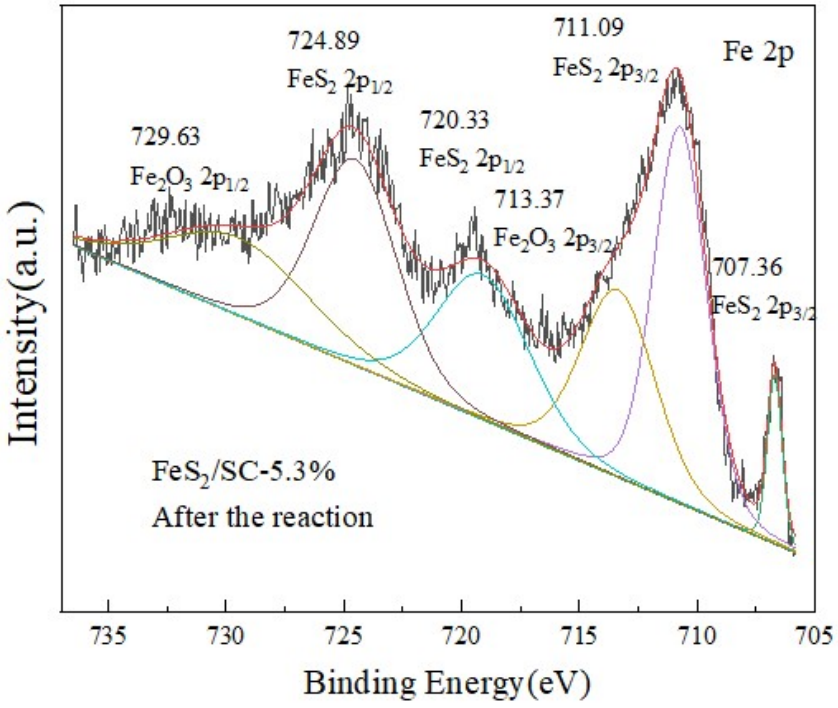

Figure S1. Fe2p XPS spectra of FeS_2/SC after the enzyme-catalyzed reaction.

Response Surface Methodology (RSM). The experimental temperature was fixed at 25 ℃, the concentrations of H_2O_2 and TMB were 60 μM and 1.2 mM, respectively, and the reaction time was 1 min. The solution pH (X_1), nanozymic dosage (μg/mL, X_2), and Ni^{2+} concentration (mM, X_3) were independent variables, the absorbance value at 652nm (A_{652nm}, y) was the dependent variable. The response surface method (RSM) based on BBD (Box-Behnken Design) was used to optimize the experimental conditions, and the second-order polynomial equation (as shown in Equ. (1)) was obtained. The reaction conditions were optimized according to the optimal solution of the equation:

$$y = 1.74 - 0.1375X_1 + 0.0478X_2 + 0.0247X_3 - 0.0169X_1X_2 - 0.0181X_1X_3 + 0.0825X_2X_3 - 0.5323X_1^2 - 0.141X_2^2 - 0.1585X_3^2 \quad (1)$$

Table S1 lists the values of X_1, X_2, and X_3. For example, A_{652nm} is the highest at pH = 4.0 among 3.0, 3.5, 4.0, 4.5, 5.0, and 5.5. So X_1 was selected for 3.5, 4.0, and 4.5. Table S1 lists the experimental and calculated results (A_{652nm}), indicating that Eq. (1) can be used as the model for the prediction experiment. The two-dimensional (2D) contour and three-dimensional (3D) surface drawings are shown in Figure S2. The individual and mutual effects among the dependent and independent variables can be reflected by two-dimensional (2D) contour lines and three-dimensional (3D) topographic maps. The two-dimensional contour lines are elliptical contour lines, indicating that the interaction is significant.[1] Figure S2A and D reflect the interaction effect of the concentration of Ni^{2+} (3.0 mM), pH, and the amount of nanozyme. A_{652nm} increases with the increase of pH and the amount of enzyme. In the contour line, the center of the ellipse is the optimal

value. It is clear from the figure that the pH is close to 3.92 and the nanozyme dosage is optimal at close to 73 μg/mL. It can be seen that this analysis method can make up for the defects of single factor experiment. Figure S2B and Figure S2E show the interaction between pH and C loading at a fixed dosage of nanozyme (70 μg/mL). Figure S2C and Figure S2F reflect the interaction effect of nano-enzyme dosage and C load on absorbance value when pH of fixed solution is 4. In order to obtain the optimal experimental conditions, the optimal solution of the second-order polynomial equation was obtained as pH 3.92, concentration of nanozyme 73 μg/mL, and concentration of Ni^{2+} 3.2 mM corresponding to $Fe_{0.75}Ni_{0.25}S_2$/SC based on the ICP results.

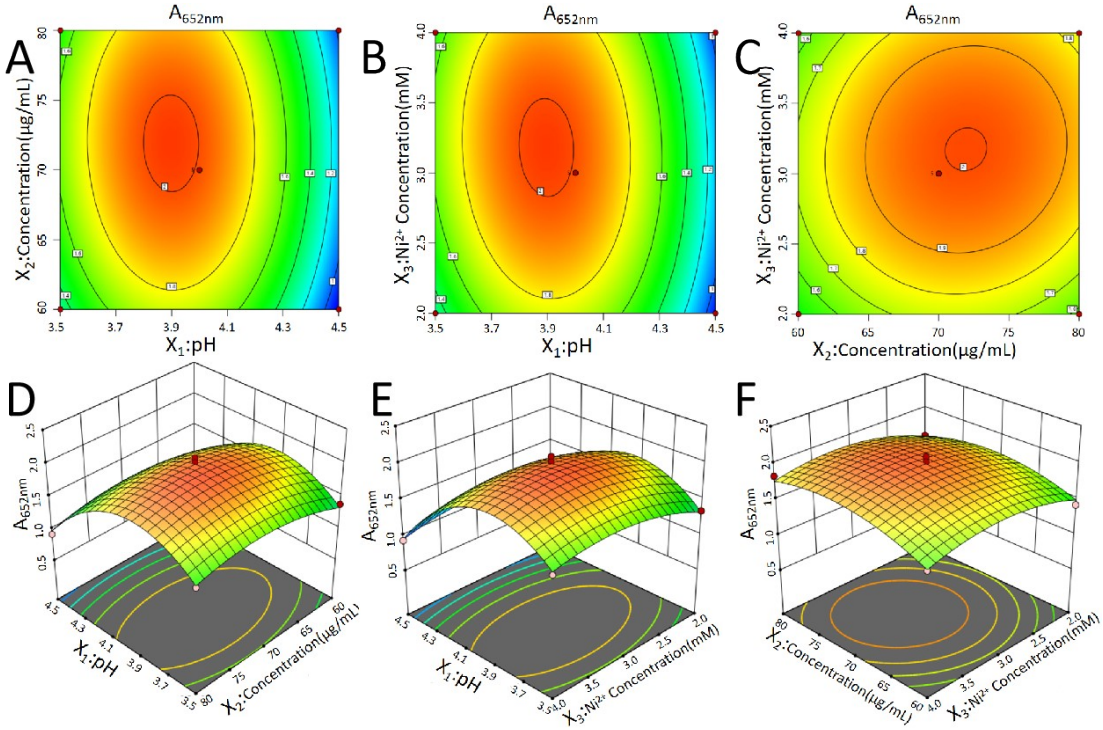

Figure S2. 2D contour diagram and 3D surface diagram of the influence of various factors on POD activity (A_{652}), (A) and (D) X_1 and X_2 (X_3 = 3.0), (B) and (E) X_1 and X_3 (X_2 = 70), (C) and (F) X_2 and X_3 (X_1 = 4.0).

Table S1. Experimental and calculated results based on Eq. (1).

Run	X_1	X_2(μg/mL)	X_3(mM)	$y(A_{652nm})$	
				Experimental	Calculated
1	3.5	80	3.0	1.48	1.51
2	4.0	70	3.0	2.02	1.99
3	4.0	80	4.0	1.83	1.76
4	4.5	80	3.0	0.92	0.97
5	4.0	70	3.0	1.99	1.99
6	4.0	60	4.0	1.54	1.55
7	4.0	60	2.0	1.42	1.49
8	4.0	70	3.0	1.91	1.99
9	4.0	70	3.0	1.95	1.99
10	4.0	80	2.0	1.59	1.58
11	3.5	70	2.0	1.34	1.32
12	4.0	70	3.0	2.09	1.99
13	3.5	60	3.0	1.38	1.33
14	4.5	70	2.0	0.95	0.91
15	3.5	70	4.0	1.49	1.53
16	4.5	60	3.0	0.89	0.86
17	4.5	70	4.0	0.93	0.94

In order to further evaluate the adequacy and significance of the model, a linear analysis was conducted on the changes between the predicted value of the model and the experimental value, and a good correlation was obtained ($R^2 = 0.9894$), with a slope of 0.98521, as shown in Figure S3A, indicating a significant model fitting.[2] In addition, the residual distribution map is also an important factor to evaluate whether the model

fitting results are significant. As shown in Figure S3B, it fits well with the straight line, indicating that there is no serious non-normality.[3] In addition, as shown in Figure S3C, no matter how the predicted value changes, the residual distribution is between -3.0 and +3.0.[3] The results show that the model can better reflect the relationship between A_{652nm} (y) and independent variables (X_1, X_2, and X_3).[4] ANOVA analysis was performed on the model, as shown in Table S2. F value is 98.05 and P value is >0.0001, indicating that the model is significant. The comparison of factor f of each variable can reflect its influence on the dependent variable (A_{652nm}). By comparing the F value of each variable factor, their influence on the dependent variable (A_{652nm}) can be reflected.[5] The results showed that the influence capacity of A_{652nm} was pH > nanozymic concentration > Ni^{2+} concentration. "Lack of Fit F-value" is 0.0078, indicating that is not significant compared to the pure error. The second-order polynomial model coefficient (R^2) and adjustment coefficient (R^2) were 0.9875 and 0.9714, respectively, indicating that the model response values were in good agreement with the experimental values.[6] The variance coefficient (C.V.%) is 4.72, indicating the model high accuracy and reliability.[6]

Table S2 ANOVA for $A_{652\ nm}$ from BBD.

Source	Sum of Squares	df	Mean Square	F-value	p-value	
Model	1.68	9	0.1867	61.31	< 0.0001	significant
X_1	0.1512	1	0.1512	49.68	< 0.0001	
X_2	0.0183	1	0.0183	6..01	0.0441	
X_3	0.0049	1	0.0049	1.60	0.2462	

X_1X_2	0.0011	1	0.0011	0.3741	0.5601	
X_1X_3	0.0013	1	0.0013	0.4316	0.5322	
X_2X_3	0.0272	1	0.0272	8.94	0.0202	
X_1^2	1.19	1	1019	391.78	< 0.0001	
X_2^2	0.0837	1	0.0837	27.50	0.0015	
X_3^2	0.1057	1	0. 1057	34.73	0.0006	
Residual	0.0213	7	0.0213			
Lack of Fit	0.0078	3	0.0078	0.7747	0.5659	not significant
Pure Error	0.0135	4	0.01335		.	
Cor Total	1.70	16				
Std. Dev.	0.0731		R^2	0.9875		
Mean	1.49		Adjusted R^2	0.9714		
C.V. %	4.72		Predicted R^2	0.9140		
			Adeq Precision	19.8895		

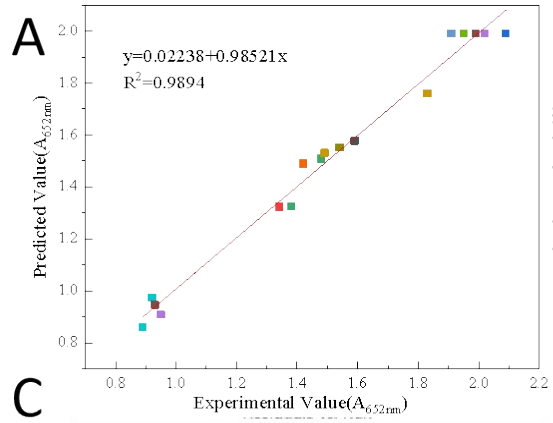

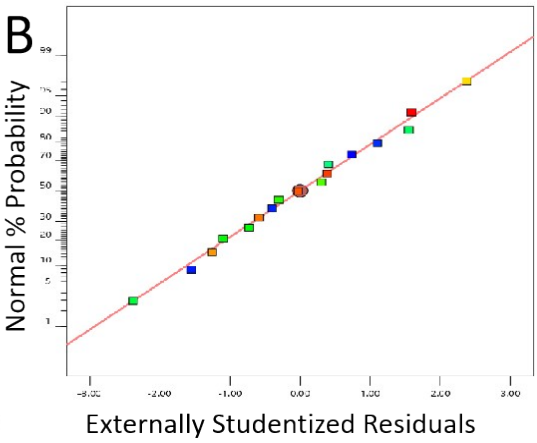

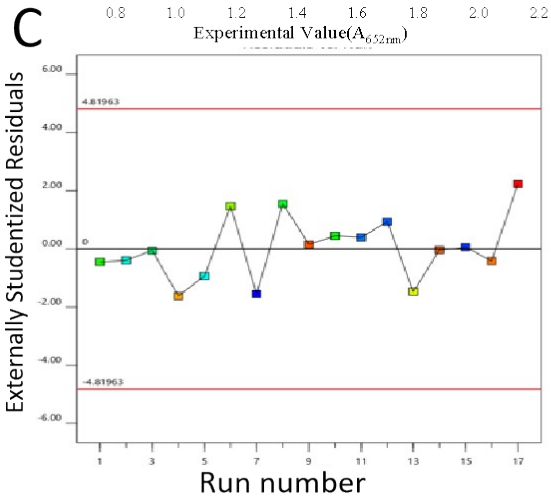

Figure S3. (A) Linear relationship between experimental and calculated values of A_{652nm},(B) Normal probability diagram of the internalized residual of A_{652nm}, and (C) running number and residual of A_{652nm}.

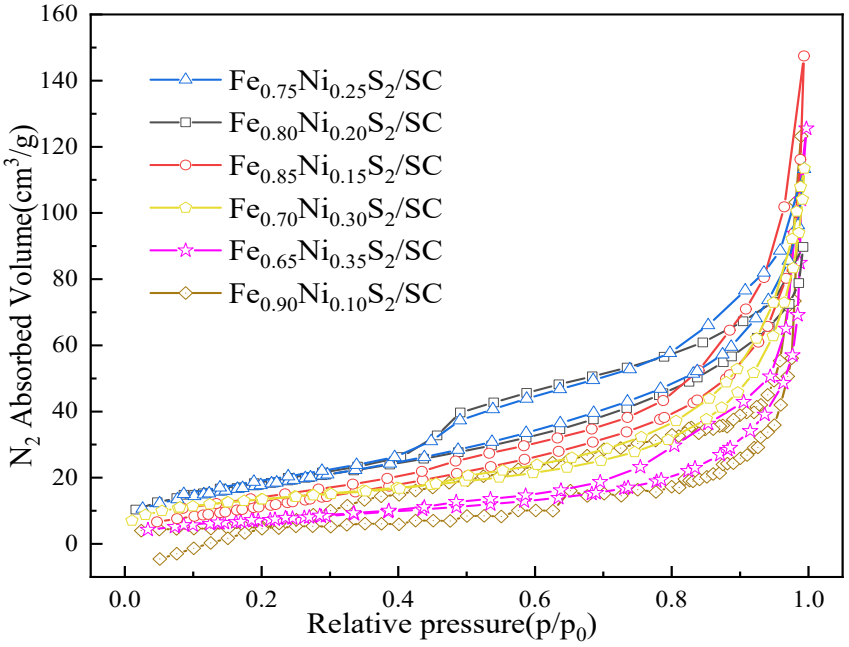

Figure S4. N_2 adsorption curves of different catalysts

The N_2 adsorption-desorption isotherms of $Fe_xNi_{1-x}S_2$/SC are shown in Figure S4, indicating porous properties of $Fe_xNi_{1-x}S_2$/SC. According to the Brunauer-Emmett-Teller model, the BET specific surface areas of these samples were obtained as shown in Table S3. These results indicate that the Ni content increasing related to the increase of the specific surface area of $Fe_xNi_{1-x}S_2$/SC ($Fe_{0.90}Ni_{0.10}S_2$/SC, $Fe_{0.85}Ni_{0.15}S_2$/SC, and $Fe_{0.80}Ni_{0.20}S_2$/SC). When the Ni content was further increased ($Fe_{0.75}Ni_{0.25}S_2$/SC and $Fe_{0.65}Ni_{0.35}S_2$/SC), the specific surface area decreased.

Table S3. BET results of $Fe_xNi_{1-x}S_2$/SC

	$Fe_{0.90}Ni_{0.10}S_2$/SC	$Fe_{0.85}Ni_{0.15}S_2$/SC	$Fe_{0.80}Ni_{0.20}S_2$/SC	$Fe_{0.75}Ni_{0.25}S_2$/SC	$Fe_{0.70}Ni_{0.30}S_2$/SC	$Fe_{0.65}Ni_{0.35}S_2$/SC
BET(m^2/g)	38.21	57.74	66.80	67.33	54.46	48.57

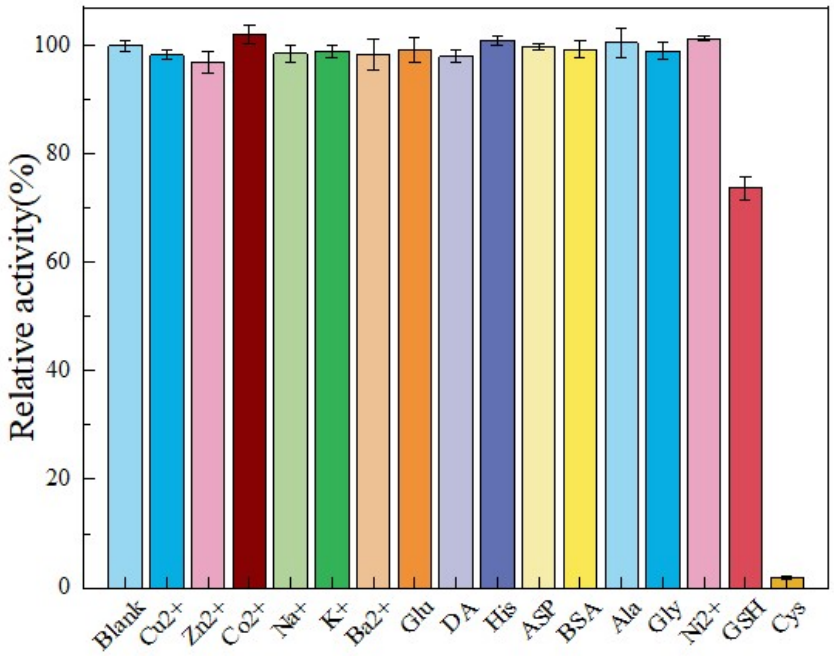

Figure S5. Effects of different interfering cations and biological macromolecules on POD-like activity of $Fe_{0.75}Ni_{0.25}S_2$/SC.

REFERENCES

[1] A. M. Roudi; S. Salem; M. Abedini; A. MaslahatiM. Imran. Response Surface Methodology (RSM)-Based Prediction and Optimization of the Fenton Process in Landfill Leachate Decolorization. *Processes*, 2021, **9**, 2284.

[2] R. Tabaraki; S. Zadkhast; A. NajafiV. R. Moghaddam. Performance and cost analysis of dye wastewater treatment by Fenton, electro-Fenton, and biosorption: Box-Behnken experimental design and response surface methodology. *Biomass. Convers. Bior.*, 2022.

[3] D. A. Aljuboury; P. Palaniandy; H. B. A. Aziz; S. Feroz. Evaluation of the solar photo-Fenton process to treat the petroleum wastewater by response surface methodology (RSM). *Environ. Earth. Sci.*, 2016, **75**, 333.

[4] S. Xin; G. Liu; X. Ma; J. GongY. Xin. High efficiency heterogeneous Fenton-like catalyst biochar modified $CuFeO_2$ for the degradation of tetracycline: Economical synthesis, catalytic performance and mechanism. *Appl. Catal. B.*, 2020, **280**, 119386.

[5] J. Chen; G. Li; H. Yong; H. Zhang; H. Zhao; T. An. Optimization synthesis of carbon nanotubes-anatase TiO_2 composite photocatalyst by response surface methodology for photocatalytic degradation of gaseous styrene. *Appl. Catal. B.*, 2012, **123-124**, 69-77.

[6] R. Hazime; Q. H. Nguyen; C. Ferronato; T. HuynhJ. M. Chovelon. Optimization of imazalil removal in the system UV/TiO_2/$K_2S_2O_8$ using a response surface methodology (RSM). *Appl. Catal. B.*, 2013, **132-133**, 519-526.